Springer

KSME

Journal of Mechanical Science and Technology 24 (12) (2010) 2555~2560
www.springerlink.com/content/1738-494x
DOI 10.1007/s12206-010-0925-z

# Effects of upper inflow area on pool boiling in vertical annulus with closed bottoms †

Myeong-Gie Kang*

*Department of Mechanical Engineering Education, Andong National University, 388 Songchun-dong, Andong-City, Kyungbuk 760-749, Korea*

(Manuscript Received June 23, 2009; Revised April 12. 2010; Accepted August 9, 2010)

**Abstract**

The upper inflow area was changed to identify its effects on the pool boiling heat transfer of saturated water at atmospheric pressure in a vertical annulus with closed bottoms. The inside surface of a 25.4 mm diameter tube was heated. The ratio between the gaps measured at the upper and lower regions of the annulus ranged from 0.18 to 1. Two different lengths of modified gap were investigated. The effects of the inflow area on heat transfer became evident as the heat flux increased and the gap ratio decreased. If the gap ratio was smaller than 0.51 and the height of the interrupter was 10 mm, a significant change in heat transfer was observed. This was attributed primarily to the formation of a lumped bubble around the upper regions of the annulus and the generation of active liquid agitation in the annular gap space.

*Keywords*: Annulus; Heat transfer; Inflow area; Pool boiling; Vertical tube

## 1. Introduction

The mechanism of pool boiling heat transfer has been studied extensively for several decades [1, 2]. Studies on the crevices can be divided into two categories: those concerning annuli [3-6] and those regarding plates [7-9]. Like geometric conditions, flow to the crevices can be controlled. Some geometries include a closed bottom [3, 6, 7].

Confined boiling, as compared with unconfined boiling, can result in heat-transfer improvements of up to 300%-800% at low heat fluxes [3, 7]. The heat-transfer coefficient increases when the gap size decreases to a certain value [2-5, 8]; any further gap size decrease, however, effects a sudden heat-transfer coefficient drop. One of the possible causes of this deterioration is the formation of large bubbles in the upper regions of the annulus [5].

Around the upper region of a closed-bottom annulus, the downward liquid flow interferes with the upward bubble flow. Thereafter, bubbles coalesce into a large lump while fluctuating up and down in the annular gap. Kang [6] published the effective results of moving the deterioration point to the higher heat flux and preventing, thereby, the occurrence of critical heat flux. He accomplished this by controlling the length of the outer tube of the annulus. The major cause of large bubble formation, which is, in turn, the cause of deterioration, is the lack of inflow through the lower regions of the annulus. Kang [10] determined that the inflow area in the bottom regions of an annulus changes heat transfer significantly, moving the deterioration point to higher heat fluxes.

Summarizing the previous work on pool boiling heat transfer in an annulus, it can be stated that heat-transfer coefficients are highly dependent on the geometry and the confinement condition. Variation of the upper inflow area changes the outward velocity of the bubbles from the annulus. It also changes the inflow velocity through the upside gap. This kind of geometry is found in in-pile test sections that, importantly, are used to identify nuclear fuel irradiation behavior under the operating conditions of commercial power plants. To the present author's knowledge, no results on this effect have as yet been published. The results of this study therefore could provide clues to the thermal design of such facilities.

## 2. Experiments

Schematic views of the experimental apparatus and test section are shown in Fig. 1. The water tank (Fig. 1(a)), composed of stainless steel, had a 950×1300 mm rectangular cross-section, a height of 1400 mm, and an 800×1000×1100 mm (depth×width×height) inner tank. Four auxiliary heaters (5 kW/heater) were installed at the space between the inside and outside tank bottoms. The heat exchanging tube was a resistance heater (Fig. 1(b)) in the form of a stainless steel tube

† This paper was recommended for publication in revised form by Associate Editor Dae Hee Lee

* Corresponding author. Tel.: +82 54 820 5483, Fax.: +82 54 823 1766
E-mail address: mgkang@andong.ac.kr

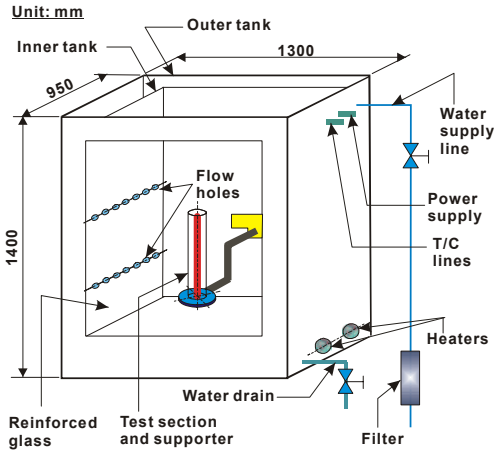


(a) water tank

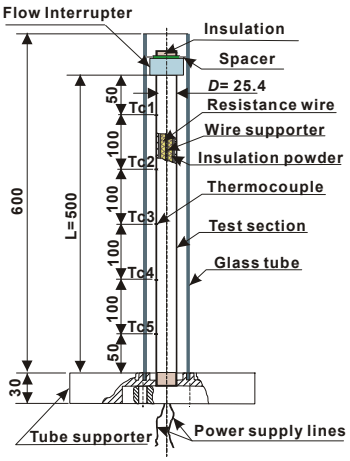


(b) assembled test section

Fig. 1. Schematic of experimental apparatus.

Table 1. Test matrix and $q''$ versus $\Delta T_{sat}$ data.

| $d$ mm | $w$ mm | $s_d$ mm | $s_r$ | $q''$ kW/m² | Geometry | Number of data |
|---|---|---|---|---|---|---|
| - | - | - | - | 0-120 | Single tube | 12 |
| 25.4 | - | 15.0 | 1 | 0-120 | Bottom closed | 12 |
| 40 | 10 | 7.7 | 0.51 | 0-120 | Bottom closed | 12 |
| 45 | 10 | 5.2 | 0.35 | 0-120 | Bottom closed | 12 |
| 50 | 10 | 2.7 | 0.18 | 0-120 | Bottom closed | 12 |
| 40 | 30 | 7.7 | 0.51 | 0-120 | Bottom closed | 12 |
| 45 | 30 | 5.2 | 0.35 | 0-120 | Bottom closed | 12 |
| 50 | 30 | 2.7 | 0.18 | 0-120 | Bottom closed | 12 |

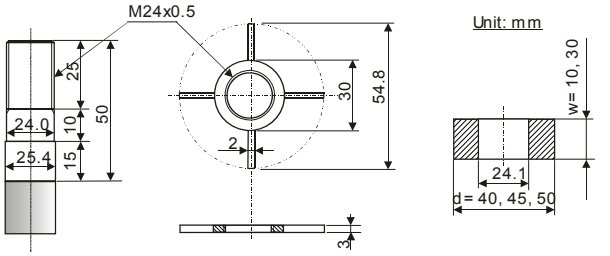


(a) test section (b) spacer (c) flow interrupter

Fig. 2. Detailed view of tube upper regions.

($L$ =0.5 m, $D$ =25.4 mm), the surface of which was buffed to a high degree of smoothness. Electric power, 220 V AC, was supplied through the bottom of the tube.

The tube outside was instrumented with five T-type sheathed thermocouples (diameter: 1.5 mm). The thermocouple tip (about 10 mm) was brazed onto the tube wall to an average thickness of less than 0.1 mm using a kind of brass. The temperature decrease along this brazing metal was calibrated by means of a one-dimensional conduction equation. The water temperatures were measured with six sheathed T-type thermocouples brazed onto a stainless steel tube placed vertically at a corner of the inside tank. All of the thermocouples were calibrated for the saturation value of 100°C, since all of the tests were conducted at atmospheric pressure. To measure and/or control the supplied voltage and current, two power supply systems were used.

For the tests, the heat exchanging tube was assembled vertically at the supporter (Fig. 1(a)), and an auxiliary supporter was used to fix a glass tube (Fig. 1(b)). To create the annular condition, a glass tube of 55.4 mm inner diameter ($D_i$) and 600 mm length was situated around the heated tube. The gap size ($s = (D_i - D)/2$) of the main body of the annulus was 15 mm. To maintain the gap size between the heated tube and the glass tube, a spacer (Fig. 2(b)) was installed in the upper region of the test section. The upper inflow into the annular space was controlled by flow interrupters (Fig. 2(c)) having outside diameters ($d$) of 40, 45, and 50 mm, respectively. After installing the flow interrupter, the spacer was screwed down tightly on the test section. The gap size around the interrupter ($s_d = (D_i - d)/2$) was different from that of the main body. The gap ratios ($s_r = s_d / s$) varied from 0.18 to 1, as shown in Table 1. The single tube is without the outer annulus. Among the values, $s_r$ =1 represents the annulus without the flow interrupter and the number of data means the arithmetic average values of the measured local temperatures.

After the water tank was filled to the initial level of 1100 mm, the water was heated by four pre-heaters running at constant power. When the water temperature reached the saturation value, the water boiled for 30 minutes, removing the dissolved air. The temperatures of the tube surfaces ($T_W$) were measured when they were in the steady state, while the heat flux on the tube surface was controlled with input power.

The heat flux from the electrically heated tube surface was calculated from the measured values of the input power as

$$q'' = \frac{VI}{\pi DL} = h_b \Delta T_{sat} = h_b (T_W - T_{sat}) \quad (1)$$

where $V$ and $I$ are the supplied voltage and current, and $D$ and $L$ are the outside diameter and length of the heated tube,

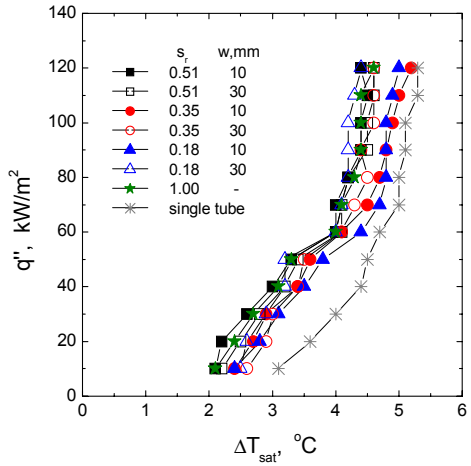


Fig. 3. Curves of $q''$ versus $\Delta T_{sat}$ data.

respectively, and $T_W$ and $T_{sat}$ represent the measured temperatures of the tube surface and the saturated water, respectively.

The uncertainties of the experimental data were calculated from the law of error propagation [11]. The data acquisition error ( $A_T$ , ±0.05°C) and the precision limit ( $P_T$ , ±0.1°C) were factored into an uncertainty analysis of the temperature. The 95%-confidence uncertainty of the measured temperature was calculated as ±0.11 °C from $(A_T^2 + P_T^2)^{1/2}$ . The error bound of the voltage and current meters used for the test was ±0.5% of the measured value. Therefore, the uncertainty in the heat flux was estimated to be ±0.7%. Since the values of the heat-transfer coefficient were derived from the calculation of $q''/\Delta T_{sat}$ , they were statistically analyzed. Taking the mean of the uncertainties of the propagation errors into consideration, the uncertainty of the heat-transfer coefficient was determined to be ±6%.

## 3. Results and discussion

Fig. 3 shows the variations in the heat transfer as $s_r$ and $w$ change. Owing to the interrupter, the heat transfer deteriorated. The smaller gap ratio and the shorter length resulted in a very significant heat-transfer change. At $w$ =10 mm, $\Delta T_{sat}$ increased 18.2% (from 4.4 to 5.2 ℃) when $s_r$ was decreased by 31.4% (from 0.51 to 0.35) at the given heat flux ( $q''$ =120 kW/m$^2$). At $w$ =30 mm however, the effect of the interrupter on the heat transfer was smaller than that for the shorter one. According to Fig. 3, $\Delta T_{sat}$ had the same value under the same conditions used for the shorter interrupter. A further decrease in the gap ratio, from 0.35 to 0.18, showed a slight decrease in $\Delta T_{sat}$ through the heat fluxes for $w$ =30 mm, or at the higher heat fluxes, more than 90 kW/m$^2$ for $w$ =10 mm. Therefore, the changes in heat-transfer mechanism depend on $s_r$ , $w$ , and $q''$ . The slope of the $q''$ versus $\Delta T_{sat}$ curve for $w$ =10 mm became smaller than that of the $w$ =30 mm annulus as $s_r$ decreased from 1 to 0.18.

However, significant improvements in heat transfer were observed in the annuli, compared with the single unrestricted tube. For the heat fluxes lower than 60 kW/m², the heat transfer for the annuli was much greater than for the single tube. The annuli with the interrupter had similar curve slopes to that of the annulus without the interrupter. As $w$ =10 mm, the curves with the interrupter were seen to merge into the curve of the single unrestricted tube when $s_r \leq 0.35$ and the heat flux increased beyond 60 kW/m². The slops of the curves for $w$ =30 mm were similar to that of the annulus without the interrupter.

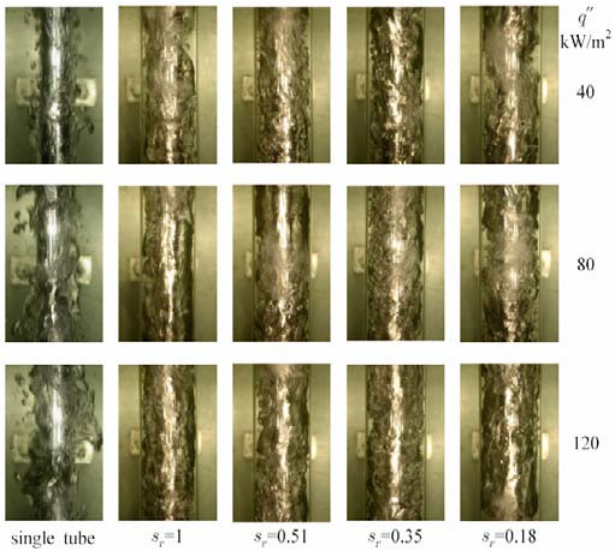


Fig. 4. Photos of pool boiling at $w$ =10 mm.

Fig. 4 shows photos of pool boiling for $w$ =10 mm. The photos are taken at around the mid-point of the tube length. The annuli show large bubbles inside the gap space. The increase in the number and size of the bubbles was observed while the interrupter was installed. Although the annuli showed no remarkable differences, the visual observation of the boiling phenomena indicated that, as the gap ratio decreased from 1 to 0.18, more frequent generation of bubble lumps was observed in the upper region of the annulus. And this was accelerated as the heat flux increased.

Changes in the average heat-transfer coefficients for the gap ratio increases are plotted in Fig. 5. When the gap ratio was less than 0.51, a sudden change in heat-transfer coefficients was observed at $w$ =10 mm regardless of the heat flux. However, at $w$ =30 mm, no such change was apparent.

To clarify the effects of the interrupter length on heat transfer, the ratios between two averaged heat-transfer coefficients for the annuli with different interrupter lengths are plotted in Fig. 6. At $s_r$ =0.51, the calculated results of $h_{b,w=30}/h_{b,w=10}$ are less than 1 regardless of the heat flux. The ratio converges to a value around 0.95 as the heat flux grows larger than 50 kW/m$^2$. At $s_r$ =0.35, the ratios of $h_{b,w=30}/h_{b,w=10}$ are larger than 1 because the heat flux is more than 40 kW/m$^2$ . These results might be attributable to the following phenomena.

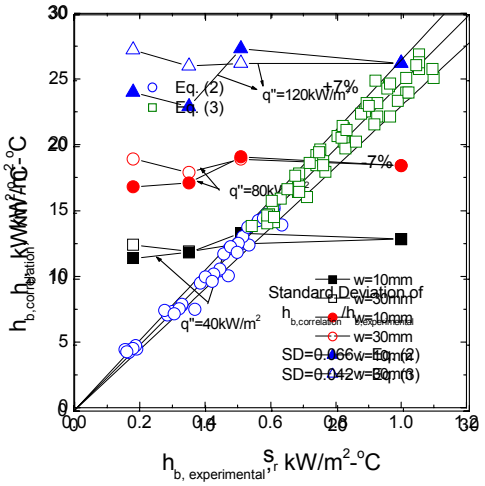


Fig. 5. Curves of $h_{b,correlation}$ versus $h_{b,experimental}$.

Fig. 8. Comparison of experimental data with calculated heat-transfer coefficients by empirical correlation.

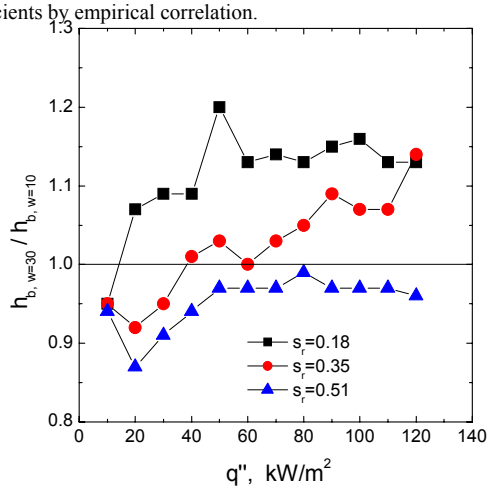


Fig. 6. Changes in heat-transfer coefficient versus heat flux.

(1) Two competing heat-transfer mechanisms can be considered. One is the reduced liquid velocity due to bubble coalescence, and the other is active liquid agitation due to pulsating flow. Velocity reduction decreases heat transfer, whereas agitation increases it.

(2) The flow interrupter obstructs the outward bubble flow from the annulus. The detached bubbles become stagnant for a while and accumulate in the upper region of the annulus. Thereafter, the upward velocity of the fluid decreases due to the bubbles. Since the major heat-transfer resistance is the heat conduction across the liquid film, the reduced film thickness under the bubbles increases the heat-transfer coefficient [3]. When the fluid velocity decreases, the shear stress on the liquid film at the heated surface decreases and, accordingly, the thickness of the liquid film increases. The thickened film decreases heat transfer. The phenomenon of decreasing heat transfer resulting from decreased fluid velocity is observed also in forced convective nucleate boiling [12].

(3) For the annuli with closed bottoms, serious interference is generated between the outward bubbles and the incoming liquid. This interference, then, disturbs the outward bubble flow and creates large lumps of bubbles in the annular space. The smaller the gap ratio, the larger the bubbles will be. If the lump flows out, a vacancy is created and, then, a sudden rush of liquid occurs. During the process, the inside fluid is accelerated, moving upward and downward, generating a pulsating flow in the gap space. As a result, very active liquid agitation is created. The high rate of heat transfer by boiling in the gap space has been ascribed to the intense agitation of the liquid at the heating surface by the bubbles [10]. If large bubble lumps are generated, a reduction in fluid velocity first occurs. Then, increased liquid agitation results. If the upper inflow area is not sufficient, the flow friction increases. The decrease in the heat-transfer rate is accelerated as the value of the gap ratio decreases.

(4) Further decreases in the gap ratio results in the generation of much larger bubbles underneath the interrupter. These lumps occupy a larger space, and finally generate stronger liquid agitation in the annular space. This tendency is also caused by the increase in the heat flux and the interrupter length. As the heat flux increases, more bubbles are generated, coalescing together to create larger bubbles. As the interrupter length is increased, stronger flow friction is created between the outward fluid and the wall than with the shorter interrupter. Thereafter, larger bubble lumps are generated and, then, increased heat-transfer coefficients are effected, followed by increased liquid agitation.

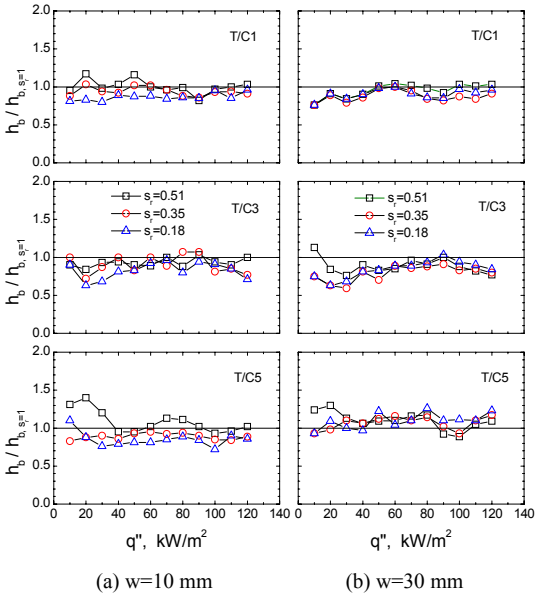


(a) w=10 mm (b) w=30 mm

Fig. 7. Local heat-transfer coefficients versus heat flux.

Local heat-transfer coefficients at the locations of thermocouples #1, #3, and #5 are shown in Fig. 7. The ratios between two heat-transfer coefficients with or without the interrupter are plotted. The ratios are almost 1 at the uppermost location (T/C1) where bubble coalescence is dominant. However, the

ratios are almost 1 at the lowermost location (T/C5) as well. At $w$ =30 mm, this tendency is more evident. At T/C5, the major heat-transfer mechanism is the intensity of liquid agitation. The generation of larger bubbles creates active pulsating flow in the space and, then, results in increased heat transfer at this location.

To obtain the parametric effects of the gap ratio and the interrupter length on heat-transfer coefficients, two empirical correlations were suggested. As listed in Table 1, a total of 84 data points were obtained for the heat flux versus the wall superheat. The value of $w_r$ (= $d/w$) for the annulus without the interrupter was taken as 1 for the convenience of correlation development. From visual observations of the boiling behavior and also from the analysis of the present experimental data, two empirical heat-transfer correlations were derived for the two different heat flux regions, in order to fit the present experimental data more closely. Using the present experimental data and a statistical analysis computer program (which uses the least square method as a regression technique), the following correlations for prediction of the average heat-transfer coefficients were derived:

$$h_b = 0.95 q''^{0.71} s_r^{0.05} w_r^{-0.01} \quad (q'' < 60 \text{ kW/m}^2) \tag{2}$$

$$h_b = 0.53 q''^{0.82} s_r^{0.01} w_r^{-0.05} \quad (q'' \geq 60 \text{ kW/m}^2) . \tag{3}$$

In the above equations, the dimensions of $h_b$ and $q''$ are kW/m²-°C and kW/m², respectively, and $s_r$ (= $s_d/s$) and $w_r$ (= $d/w$) are dimensionless. The equations are valid for $10 \leq q'' \leq 120$ kW/m²-°C, $0.18 \leq s_r \leq 1$, and $0.85 \leq w_r \leq 5$. Since the annular height can change heat-transfer coefficients, the equation is applicable only to annuli of similar height.

To confirm the validity of the empirical correlations, statistical analyses of the ratios between the calculated and the measured heat-transfer coefficients were performed. The standard deviations were 0.066 and 0.042 for $q''$ <60 kW/m$^2$ and $q''$ ≥60 kW/m$^2$, respectively. A comparison between the heat-transfer coefficients from the tests and the correlations is shown in Fig. 8. The scattering bounds of the present experimental data, obtained from the fitted curves of Eqs. (2) and (3), were ±7%, with some exceptions. Therefore, it can be stated that the developed correlations predict the data within a reasonable error bound.

## 4. Conclusions

To investigate the effects of the upside inflow area on pool boiling heat transfer in a vertical annulus with closed bottoms, the gap size at the upper region of the annulus was regulated. For the test, a heated tube of 25.4 mm diameter and water at atmospheric pressure were used. The major conclusions of the study are as follows:

(1) Adoption of a flow interrupter for an annulus generally decreases heat-transfer coefficients compared with the case without a flow interrupter. For $s_r$ <0.51 and $w$ =10 mm, a noticeable decrease in heat-transfer coefficients was observed. However, if the height of the interrupter was increased, no noticeable change in heat transfer was observed.

(2) The causes of the heat-transfer change are recognized as the reduced fluid velocity and active liquid agitation resulting from the generation of large bunches of bubbles underneath the flow interrupter.

(3) To quantify the effects of the upside narrower gaps on heat transfer, two empirical correlations predicting the experimental data within a reasonable error bound were derived. According to the correlations, the heat-transfer coefficients were proportional to $s_r^{0.05}$ and $w_r^{-0.01}$ at $q''$ <60 kW/m$^2$ and to $s_r^{0.01}$ and $w_r^{-0.05}$ at $q''$ ≥60 kW/m$^2$.

## References


[1] M. H. Chun and M. G. Kang, Effects of heat exchanger tube parameters on nucleate pool boiling heat transfer, *ASME J. Heat Transfer*, 120 (1998) 468-476.

[2] M. Shoji, Studies of boiling chaos: a review, *Int. J. Heat Mass Transfer*, 47 (2004) 1105-1128.

[3] S. C. Yao and Y. Chang, Pool boiling heat transfer in a confined space, *Int. J. Heat Mass Transfer*, 26 (1983) 841-848.

[4] Y. H. Hung and S. C. Yao, Pool boiling heat transfer in narrow horizontal annular crevices, *ASME J. Heat Transfer*, 107 (1985) 656-662.

[5] M. G. Kang and Y. H. Han, Effects of annular crevices on pool boiling heat transfer, *Nuclear Engineering and Design*, 213 (2002) 259-271.

[6] M. G. Kang, Pool boiling heat transfer on a vertical tube with a partial annulus of closed bottoms, *Int. J. Heat Mass Transfer*, 50 (2007) 423-432.

[7] J. Bonjour and M. Lallemand, Flow patterns during boiling in a narrow space between two vertical surfaces, *Int. J. Multiphase Flow*, 24 (1998) 947-960.

[8] Y. Fujita, H. Ohta, S. Uchida and K. Nishikawa, Nucleate boiling heat transfer and critical heat flux in narrow space between rectangular spaces, *Int. J. Heat Mass Transfer*, 31 (1988) 229-239.

[9] J. C. Passos, F. R. Hirata, L. F. B. Possamai, M. Balsamo and M. Misale, Confined boiling of FC72 and FC87 on a downward facing heating copper disk, *Int. J. Heat Fluid Flow*, 25 (2004) 313-319.

[10] M. G. Kang, Pool boiling heat transfer in a vertical annulus as the bottom inflow area changes, *Int. J. Heat Mass Transfer*, 51 (2008) 3369-3377.

[11] H. W. Coleman and W. G. Steele, *Experimentation and Uncertainty Analysis for Engineers*, 2nd Ed., John Wiley & Sons (1999).

[12] W. M. Rohsenow, A method of correlating heat-transfer

data for surface boiling of liquids, *ASME J. Heat Transfer*, 74 (1952) 969-976.

**Myeong-Gie Kang** received his B.S. degree in Precision Mechanical Engineering from Pusan National University, Korea, in 1986. He then earned his M.S. and Ph.D. degrees from KAIST in 1988 and 1996, respectively. Dr. Kang currently is a Professor in the Department of Mechanical Engineering Education at Andong National University in Andong, Korea. He served as an engineer and researcher at KEPCO for 7 years. His research interests include pool boiling heat transfer, flow-induced vibration, and nuclear thermo-hydraulics.